Rock Mech. Rock Engng. (1994) 27 (4), 209–234

Rock Mechanics
and Rock Engineering
© Springer-Verlag 1994
Printed in Austria

Modeling of Subsidence and Stress-Dependent Hydraulic Conductivity for Intact and Fractured Porous Media

By

M. Bai[1] and **D. Elsworth**[2]

[1] Rock Mechanics Research Center, University of Oklahoma, Norman, U.S.A.
[2] Department of Mineral Engineering, Pennsylvania State University, University Park, U.S.A.

Summary

This study investigates the changes in deformation and stress dependent hydraulic conductivities that occur as a result of underground mining in intact and fractured porous media. The intact porous medium is assumed to be comprised of regularly packed spherical grains of uniform size. The variation in grain size or pore space due to the effect of changing intergranular stresses results in a change in rock hydraulic conductivity. A model is developed to describe the sensitivity of hydraulic conductivity to effective stresses through Hertzian contact of spherical grains. The fractured porous medium is approximated as an equivalent fracture network in which a single fracture is idealized as a planar opening having a constant equivalent thickness or aperture. Changes in fracture aperture as a result of changes in elastic deformation control the variation of hydraulic conductivity. A model is presented to illustrate the coupling between strain and hydraulic conductivity. Subsidence induced deformations that result from mining induced changes in hydraulic conductivity in both intact and fractured media. These changes are examined and compared with results from a mining case study.

1. Introduction

For flow within a single capillary, or by superposition through a bundle of capillaries, hydraulic conductivity, K, may be defined proportionally to a characteristic length representative of hydraulic radius, which may be expressed as

$$K = \frac{cd^2}{F(n)}\left(\frac{\rho g}{\mu}\right), \tag{1}$$

where d is the "hydraulic radius" and is related to the grain diameter or pore dimension, $F(n)$ is the porosity factor, c is a constant associated with grain packing and grain shape configuration, ρ is the fluid density, g is the gravitational acceleration and μ is the dynamic viscosity of the fluid.

Various attempts have been made to provide some insight into the physical processes represented by Eq. (1) with substantial experimental work having been completed to further verify the expression (Hubbert, 1940; Scheidegger, 1957; Kozeny, 1927; Krumbein and Monk, 1943). Also related to Eq. (1), hydraulic radius is controlled by changes in effective or intergranular stresses (De Wiest, 1969). Young et al. (1964) showed that an increase in stress acting on samples of argillaceous rocks produced a decrease in permeability of more than an order of magnitude over the results of unconfined tests. In correlating confining stresses with hydraulic conductivity, the interaction between stresses and fluid pressures (i.e. effective stress law) has been intensively investigated (Brandt, 1955; Gangi, 1978; Walsh, 1981; Gale, 1982; Barton et al., 1985; Jones, 1975), in which one of the major indeterminates is the exact magnitude of effective stress (Terzaghi, 1923; Walsh, 1981; Skempton, 1960; Geertsma, 1957; Nur and Byerlee, 1971; Robin, 1973). A review of the methodology for determining stress-dependent hydraulic conductivities is given in the Appendix.

For the purpose of predicting the change in hydraulic properties in intact porous media, this study introduces a model to describe the coupled steady flow problem using a finite element formulation. Changes in hydraulic conductivity are evaluated using the concept of elastic contact through change in grain size (or pore size). The significant influence of effective stresses in the modification of hydraulic conductivities is demonstrated.

In many cases, rock masses contain natural fractures, and both mechanical and hydraulic behavior is controlled by the presence of these features. Where groundwater moves nearly exclusively through interconnected fractures the system may be represented as an equivalent fracture network. Conceptualization of flow in a single fracture can be addressed through the parallel plate analog where a fracture is idealized as a planar opening having a constant thickness or aperture (Louis, 1969; Bear, 1972; Iwai, 1976; Hoek and Bray, 1977). Neglecting turbulent flow and assuming only flow within the fracture network, the hydraulic conductivity of a set of parallel fractures of spacing, s, is given as (e.g. Louis, 1969)

$$K = \frac{\rho g b^3}{12 s \mu}, \tag{2}$$

where b is initial fracture aperture and, s is fracture spacing.

Where the interconnection between fractures is sufficiently distributed, the network may be further idealized as an equivalent porous continuum. This piecewise continuum is represented by an equivalent anisotropic hydraulic conductivity, controlled by fracture spacing and mean aperture. The utility of this idealization is that strain-induced changes in fracture aperture, and corresponding modification of the hydraulic conductivity components, may be readily evaluated.

In this paper models for evaluation of the subsidence and stress-dependent changes in hydraulic conductivity in both intact and fractured media are discussed. Their utilities are examined in an actual mining case study. The corresponding results, calculated from models, are analyzed and compared with field measurements. The steady state models presented here are useful in quantifying the long-term influence on the groundwater regime as a result of mining.

2. Governing Equations

Assuming strains, ϵ_{ij} to be linearly related to total stresses, σ_{ij}, through pore pressure magnitude, p, enables a constitutive relation to be expressed as (Biot, 1941)

$$\epsilon_{ij} = \frac{1+\nu}{E}\sigma_{ij} - \frac{\nu}{E}\sigma_{kk}\delta_{ij} - \frac{1}{3H}p\delta_{ij} \tag{3}$$

where the mean stress may be calculated by $\sigma_{kk}/3 = trace(\sigma_{ij}/3)$, δ_{ij} is Kronecker's delta and repeated indices indicate summation. The effective modulus of Biot (1941) is given as H and E, and ν are drained elastic modulus and Poisson ratio, respectively.

The equilibrium equation, in the absence of body forces, and inertial effects may be expressed as

$$\sigma_{ij,j} = 0, \tag{4}$$

where a comma represents partial differentiation with respect to the following index. The strain displacement relationship is

$$\epsilon_{ij} = \tfrac{1}{2}(u_{i,j} + u_{j,i}), \tag{5}$$

where u_i is displacement in the x_i direction. Substituting Eqs. (3) and (5) into (4), results in the field equations of poroelasticity for the solid phase as

$$\frac{E}{2(1+\nu)}u_{i,jj} + \frac{E}{2(1+\nu)(1-2\nu)}u_{k,ki} + \alpha p_{,i} = 0, \tag{6}$$

where the pressure coefficient α is defined as (Nur and Byerlee, 1971)

$$\alpha = 1 - \frac{K_s}{K_g}, \tag{7}$$

where K_s is bulk modulus of the porous medium and K_g is bulk modulus of the grains.

Darcy's velocity, v_i, may be expressed as

$$\nu_i = -Kp_{,i}, \tag{8}$$

where K is hydraulic conductivity. The steady state continuity equation is

$$\nu_{i,i} = 0. \tag{9}$$

Combining Eq. (8) with (9) enables the field equation to be determined for the fluid phase as

$$\nabla(K\nabla p) = 0 \tag{10}$$

where ∇ is the del operator, and the steady state is of interest.

Together, Eqs. (6) and (10) represent the governing equations for the steady state coupled flow-deformation behavior.

3. Finite Element Discretization

Eqs. (6) and (10) may be used to form finite element statements for the steady

poroelastic problem, where interpolation functions are substituted to interpolate dependent nodal variables of displacements, u, and pressure, p, over individual elements. From this substitution, and use of the variational principle, the following matrix relationship is obtained:

$$\begin{pmatrix} \mathbf{F} \\ \mathbf{Q} \end{pmatrix} = \begin{pmatrix} \mathbf{G_s} & \mathbf{R_c} \\ \mathbf{0} & \mathbf{G_f} \end{pmatrix} \begin{pmatrix} \mathbf{u} \\ \mathbf{p} \end{pmatrix} \tag{11}$$

where

$$\begin{aligned} \mathbf{G_s} &= \int_V \mathbf{B}^T \mathbf{D} \mathbf{B} dV \\ \mathbf{G_f} &= \int_V \mathbf{A}^T \mathbf{K} \mathbf{A} dV \\ \mathbf{R_c} &= \int_V \mathbf{B}^T \mathbf{m} \mathbf{N} dV \\ \mathbf{F} &= \int_S \mathbf{N} \mathbf{f_i} \mathbf{dS} \\ \mathbf{Q} &= \int_S \mathbf{N} \mathbf{q} \mathbf{dS} \end{aligned} \tag{12}$$

where $\mathbf{u} = (u_1, u_2)$, $\mathbf{m} = (1\ 1\ 0)^T$, $\mathbf{B}$ is the strain-displacement matrix, $\mathbf{D}$ is the elasticity matrix, and $\mathbf{K}$ is the conductivity matrix, $\mathbf{N}$ is a vector of element shape functions, $\mathbf{A}$ contains the derivatives of the shape functions, $\mathbf{F}$ is a vector of applied boundary tractions $\mathbf{f}$, $\mathbf{Q}$ is a vector of prescribed nodal fluxes $\mathbf{q}$, and V is the volume of the domain. The sub-matrix, $\mathbf{R_c}$, of Eq. (11), represents the influence of seepage forces on the resulting deformation field.

After obtaining the displacement and pressure fields from Eq. (11), stresses can be reevaluated through Eqs. (5) and (3). The effective stresses σ_e can then be determined through the relationship

$$\sigma_e = \sigma_c - \alpha p, \tag{13}$$

where σ_c is the mean stress evaluated by $\sigma_c = \sigma_{kk}/3$ and σ_{kk} is the total stress in Eq. (3).

4. Change in Hydraulic Conductivity for Intact Rock

Through experimental investigation, Hubbert (1940) substantiated Eq. (1) by presenting the relationship

$$K = Nd^2 \left(\frac{\rho g}{\mu} \right), \tag{14}$$

where K is hydraulic conductivity, N is a dimensionless number associated with grain shape and packing, d is a size factor related either to the dimensions of the opening in the medium (pore space) or expressed as a mean size of the grain (Krumbein and Monk, 1943). In addition, d can also be some function of the

square root of the permeability k (Freeze and Cherry, 1979). In this study, d is defined as the reciprocal of the specific surface which is the ratio of bulk volume to internal area of the porous medium (Kozeny, 1927).

To express hydraulic conductivity as a function of stress conditions, Gangi (1978) derived an equation based on Hertzian contact theory (Hertz, 1895), which may be expressed as

$$K = K_0 \left\{ 1 - \frac{1}{2} \left(\frac{\Delta\sigma_c + \Delta\sigma_i}{E_0} \right)^{2/3} \right\}^4, \tag{15}$$

where σ_i is the equivalent cementing pressure; E_0 is the effective modulus of grains, and σ_c is the confining stress, given in Eq. (13). This relationship identifies an inverse proportionality between hydraulic conductivity and effective stresses. Experimental investigation of the coupling between the hydraulic conductivity and stresses was also completed by Gale (1982) and by Barton et al. (1985).

The resulting system of nonlinear Eqs. (11) may be linearized using a magnitude of hydraulic conductivity, K, that is representative of the effective stress conditions. An attempt is made in the following to evaluate the stress dependent variation in hydraulic conductivity of intact porous media, which is different from Gangi's approach in the following aspects: (a) The change in hydraulic conductivity is due to the variation of mean grain size instead of pore dimension. (b) A cubic grain packing model is adopted instead of a triangular grain packing model. (c) Pore pressure is incorporated in the formulation and is coupled with confining stress to form effective stress.

In accordance with Eq. (14), hydraulic conductivity is directly proportional to the square of mean grain diameter. It is possible to deduce from Eq. (14) that

$$K \propto R^2, \tag{16}$$

where R is grain radius.

A simple cubical grain packing structure is assumed for the porous medium as illustrated in Fig. 1. To apply Eq. (14) with this cubical packing model, we obtain the term Nd^2 from Kozeny's theory (Scheidegger, 1957) as

$$Nd^2 = \frac{1}{2} \left\{ \frac{(2R)^3}{4\pi R^2} \right\}^2 = \frac{2}{\pi^2} R^2. \tag{17}$$

In the unconsolidated state, the hydraulic conductivity can, therefore, be expressed according to Eq. (14) as

$$K = \frac{2}{\pi^2} R^2 \left(\frac{\rho g}{\mu} \right). \tag{18}$$

If the initial hydraulic conductivity K_0 is known, then the grain radius R_0 may be estimated from Eq. (18) as

$$R_0 = \pi \sqrt{\frac{K_0 \mu}{2\rho g}}. \tag{19}$$

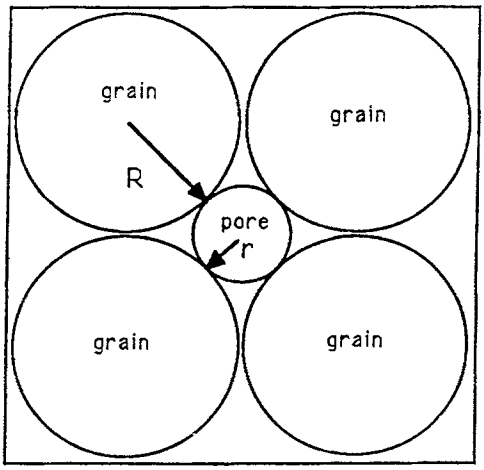

Fig. 1. Cubical packing of grains

Under uniform compression, the change in grain size within a cubical packing can be determined by analyzing the elastic contact of spheres. It is assumed that the grains of the porous medium are subjected to an effective compressive stress σ_e. Since compression is assumed to be uniform over the boundary and without the introduction of shear stress, it is sufficient to investigate only a single representative spherical contact as demonstrated in Fig. 2.

Applying the methodology introduced by Timoshenko (1934), the change of

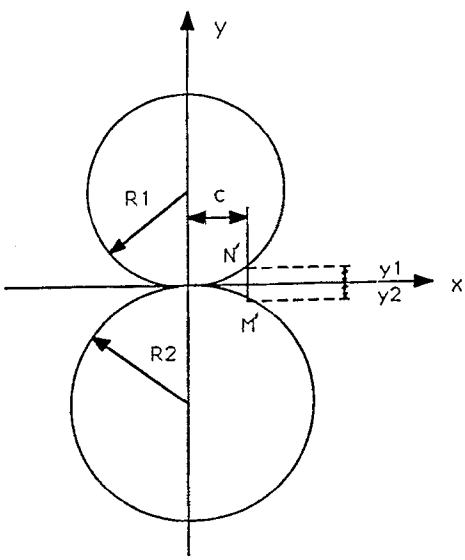

Fig. 2. Configuration of spherical contact

grain radius can be represented as

$$\Delta R = R_0 \left\{ 1 - \frac{1}{2} \left[\frac{9(1-\nu^2)}{2} \left(\frac{\pi \Delta\sigma}{E} \right)^2 \right]^{1/3} \right\}. \tag{20}$$

With consideration of the initial state, substituting Eq. (19) into (20), yields

$$\Delta R = \pi \sqrt{\frac{K_0 \mu}{2\rho g}} \left\{ 1 - \frac{1}{2} \left[\frac{9(1-\nu^2)}{2} \left(\frac{\pi \Delta\sigma}{E} \right)^2 \right]^{1/3} \right\}. \tag{21}$$

With reference to Eqs. (18) and (21), the change in hydraulic conductivity may be evaluated as

$$\Delta K = \frac{2}{\pi^2} (\Delta R)^2 \left(\frac{\rho q}{\mu} \right), \tag{22}$$

or, from Eq. (21)

$$\Delta K = K_0 \left\{ 1 \mp \frac{1}{2} \left[\frac{9(1-\nu^2)}{2} \left(\frac{\pi \Delta\sigma}{E} \right)^2 \right]^{1/3} \right\}^2, \tag{23}$$

where a negative sign refers to compressional loading and a positive sign corresponds to dilatational loading. The dimensionless hydraulic conductivity may be written as

$$\frac{\Delta K}{K_0} = \left\{ 1 \mp \frac{1}{2} \left[\frac{9(1-\nu^2)}{2} \left(\frac{\pi \Delta\sigma}{E} \right)^2 \right]^{1/3} \right\}^2. \tag{24}$$

5. Change in Hydraulic Conductivity for Fractured Rock

To determine fracture hydraulic conductivity, we assume an idealized regularly spaced fracture system as illustrated in Fig. 3. If the fracture opening is estimated from direct measurements or from pressure/flow relationships, then fracture hydraulic conductivity in the direction parallel to each fracture set may be calculated directly from the parallel plate analog (Snow, 1968; Louis, 1969) as defined in Eq. (2).

A heterogeneous porous medium containing two types of porosity (fractures and pores) may be idealized as a dual porosity medium as represented by Warren and Root (1963). Where fracture flow dominates, and only the steady condition is desired, the behavior of this dual porosity system reduces to that of an equivalent single porosity formulation.

Assuming that the individual fractures are distinctly soft with respect to the porous medium, then the deformation modified hydraulic conductivity may be

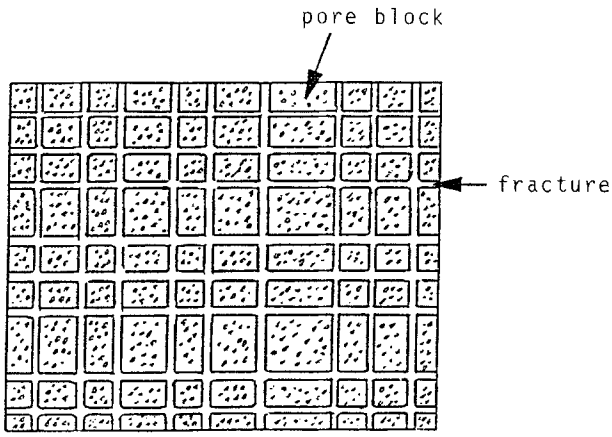

Fig. 3. Model of fractured media

written from Eq. (2) as (Elsworth, 1989)

$$\Delta K = \frac{\rho g}{12 s \mu}(b + s\Delta\epsilon)^3, \tag{25}$$

where $\Delta\epsilon$ is the body strain perpendicular to the fracture set.

The limiting condition for this expression must be controlled on physical grounds as

$$(b + s\Delta\epsilon)^3 \geqslant 0 \tag{26}$$

eliminating the possibility of overclosure of the fractures.

When the compliance of the elastic matrix approaches that of the fracture, the modulus of the matrix must be included in the evaluation of conductivity variation. Total displacements are the sum of the elastic displacements in the matrix and across the fracture (shear displacement and dilatation are neglected). The total displacement Δu_t resulting from a change in stress, $\Delta\sigma$, is given as

$$\Delta u_t = \Delta u_s + \Delta u_f = \left(\frac{s}{E} + \frac{1}{K_n}\right)\Delta\sigma, \tag{27}$$

where Δu_s and Δu_f are the displacements of the solid and the fracture, respectively, and K_n is the normal stiffness of the fracture (Fig. 4).

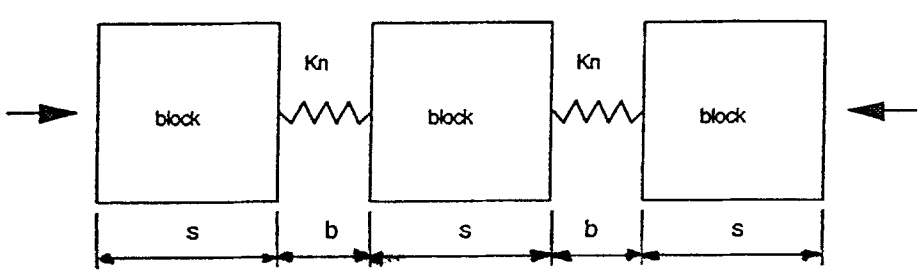

Fig. 4. A simple fracture-block mechanism, (s) spacing, (b) aperture, (Kn) fracture stiffness

The displacement across the fracture can be evaluated from Eq. (27) as

$$\Delta u_f = \Delta\epsilon\left(\frac{K_n}{E} + \frac{1}{s}\right)^{-1}, \tag{28}$$

where $\Delta\epsilon$ is the total body strain.

The modified hydraulic conductivity of a single fracture set that incorporates solid deformation may be calculated using

$$\Delta K = \frac{\rho g b^3}{12 s\mu}\left[1 + \Delta\epsilon\left(\frac{K_n b}{E} + \frac{b}{s}\right)^{-1}\right]^3. \tag{29}$$

Written in dimensionless form this expression is

$$\frac{\Delta K}{K_0} = \left[1 + \Delta\epsilon\left(\frac{K_n b}{E} + \frac{b}{s}\right)^{-1}\right]^3. \tag{30}$$

A comparison between Eqs. (2) and (30) indicates that the effect of induced strains are controlled by the dimensionless terms "$(K_n b)/E$") and "b/s". Hydraulic conductivity is little influenced when these terms are individually, or collectively, very large.

The deformation-induced enhancement of hydraulic conductivity can be calculated by using Eq. (29) where body strains are evaluated from the finite element analysis. In many cases, the in-situ hydraulic conductivity is available, as a result, the initial fracture aperture can then be estimated from rearranging Eq. (2) to give

$$b_0 = \left(\frac{12 s K_0 \mu}{\rho g}\right)^{1/3}. \tag{31}$$

The remaining task before calculating conductivity is to determine the fracture stiffness, K_n. A variety of laboratory measurement techniques are available (e.g. Einstein and Dowding, 1981). As an approximation, the normal fracture stiffness may be determined through single joint tests. From available information the ratio of fracture stiffness to elastic modulus, K_n/E, is highly variable but a subset of results (Iwai, 1976; Rosso, 1976; Witherspoon et al., 1980) suggests that reasonable magnitudes are of the order 0.1/cm (0.04/in).

Incorporation of shear displacement and strains may be made in accurately representing behavior where the fractures possess a shear rigidity characterized by their shear stiffness K_{sh}. Fracture roughness requires that dilatation accompanies any shear displacement and increases the aperture of the fractures. The displacement across the fracture due to shear strain can be calculated by the following equation (Elsworth and Xiang, 1989)

$$\Delta u_{sh} = \Delta\gamma\left(s + \frac{G}{K_{sh}}\right), \tag{32}$$

where $\Delta\gamma$ is the shear strain, K_{sh} is the shear stiffness, G is the shear modulus, and s is the fracture spacing.

Assuming that dilatation occurs instantaneously with shear initiation, and considering the change in normal stress resulting from shear displacement, the modified dimensionless hydraulic conductivity may be defined as

$$\frac{\Delta K}{K_0} = \left[1 + \Delta\epsilon\left(\frac{K_n b}{E} + \frac{b}{s}\right)^{-1} + \Delta\gamma\left(s + \frac{G}{K_{sh}}\right)(\tan\phi_d)\right]^3, \tag{33}$$

where ϕ_d is the dilatational angle. Clearly, changes in hydraulic conductivities are affected by both normal and shear strains.

6. Comparative Analysis

It is of interest to provide a qualitative comparison between the proposed stress-dependent hydraulic conductivity expounded in Eq. (24), that derived by Gangi (Eq. (15)), and also that applied to fractured media (Eq. (30)).

Assuming strain can be expressed as

$$\Delta\epsilon = \frac{\Delta\sigma}{E} = \frac{\Delta\sigma_c + \Delta\sigma_i}{E_0}, \tag{34}$$

then Gangi's method in Eq. (15) may be reformulated as

$$\frac{\Delta K}{K_0} = \{1 - \tfrac{1}{2}(\Delta\epsilon)^{2/3}\}^4, \tag{35}$$

while the proposed method for flow in intact rock described by Eq. (24), for compressive strain with $\nu = 0.25$, can be written as

$$\frac{\Delta K}{K_0} = \{1 - 1.733(\Delta\epsilon)^{2/3}\}^2 \tag{36}$$

and the proposed method for flow in a fractured medium, described in by Eq. (30), may be represented as

$$\frac{\Delta K}{K_0} = \{1 - 16.667(\Delta\epsilon)\}^3, \tag{37}$$

where it is assumed that $K_n/E = 0.1/\text{cm}$, $b = 10^{-3}\,\text{m}$, $s = 50\,\text{m}$.

A comparison of Eqs. (35) to (37) is shown in Fig. 5, in response to the variation of conductivity (K/K_0) versus strain $\Delta\epsilon$. At large strain values, the proposed method of representing intact rock yields a more drastic change in conductivity than that predicted by Gangi's formula (Gangi, 1978). As a result of the more nucleated distribution of porosity, the conductivity behavior of the fracture model is the most sensitive.

For a tensile strain field applied to the fracture flow model, and using the previously assumed parameters, the resulting change conductivity is given as

$$\frac{\Delta K}{K_0} = (1 + 16.667\Delta\epsilon)^3, \tag{38}$$

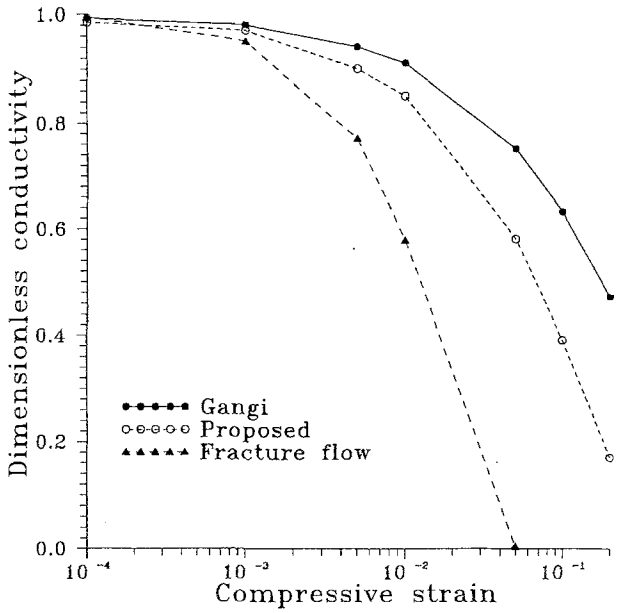

Fig. 5. Compressive strain versus dimensionless conductivity

while Eq. (24) may be correspondingly written for tensile strain as

$$\frac{\Delta K}{K_0} = [1 + 1.733(\Delta\epsilon)^{2/3}]^2. \tag{39}$$

Comparing Eqs. (38) to (39), and assuming that the modification in dimensionless hydraulic conductivity is solely controlled by the change in strata deformation, then, as expected, the conductivity of the fractured medium is considerably more sensitive to changes in strain than the intact medium as shown in Fig. 6, particularly when the strain magnitude becomes increasingly large.

From these analyses it is apparent that an increase in effective stress results in a decrease in hydraulic conductivity and vice versa (Fig. 5). This tendency has been supported by many experimental studies (Kranz et al., 1979; Witherspoon et al., 1980). This trend is reversed in the case of dilatation, as illustrated in Fig. 6.

7. Model Application: A Case Study

The validity of the proposed models may be examined by applying them to data from a mining case study. All original data, cited in the following, are referenced to the paper by Hasenfus et al. (1988).

The mine is located in West Virginia and exploits the Pittsburgh seam. The shallow water bearing strata present at the site exhibit perched or semi-perched aquifers with interbedded low permeability shales and claystones leading to a decrease in hydraulic conductivity with depth. Water level fluctuations in the

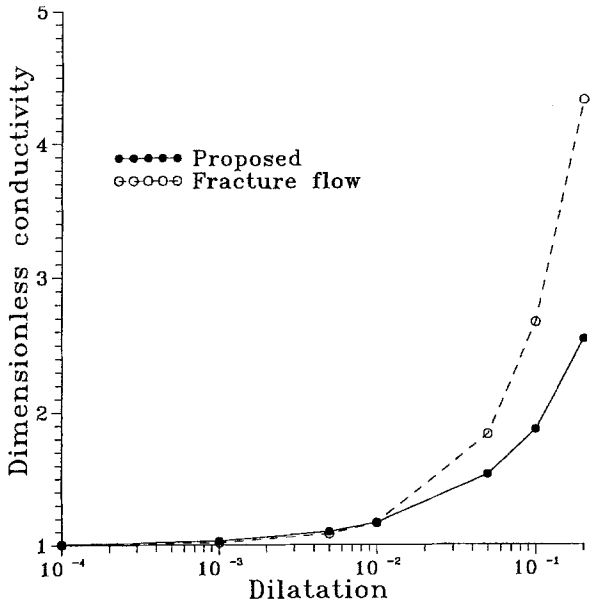

Fig. 6. Dilatation versus dimensionless conductivity

shallow aquifers are primarily attributed to the steep topography. Water levels below 400 feet (122 m) remained fairly constant throughout the pre-mining period.

The main aquifer, comprised of sandstone, is located approximately 110 to 130 feet (33.5 to 39.6 m) beneath the surface. In general, for the upper 400 feet (122 m) of overburden, hydraulic conductivity decreases with depth (Hasenfus et al., 1988). Pre-mining hydraulic conductivities for this aquifer, and a secondary aquifer located at a depth of 160 to 170 ft (48.8 to 51.8 m) below the surface, were determined through pumping tests. The normalized pre-mining hydraulic conductivity is shown in Fig. 7.

The mined seam lies directly beneath about 200 feet (61 m) of highly competent limestone and sandstone strata as contrasted with the low strength shales and claystones close to the surface (Fig. 8). The average extraction thickness was 5.75 feet (1.75 m). The mined panel was 600 feet (182.9 m) wide by 7200 feet (2194.6 m) long, and affected by two adjacent panels. Headgate development was 250 feet (76.2 m) wide and the tailgate was 225 feet (68.6 m) wide (refer to Fig. 9 of mine panel layout). The coal seam is approximately 710 feet (216.4 m) deep at the mine.

A finite element model was used to represent mining at the site. The model comprises 6 strata of 7 different elastic properties. All the materials are assumed to be isotropic. The material constants are listed in Table 1. Utilizing the symmetry of the system, the design of the finite element domain, along with all stress and pressure boundary conditions, is shown in Fig. 10 (illustrating the half profile of the mining geometry). A constant fluid pressure boundary condition is applied on the surface and around the mining panel (free drainage). The constant flux (no flow) boundary condition is employed on the side and along the base of the model,

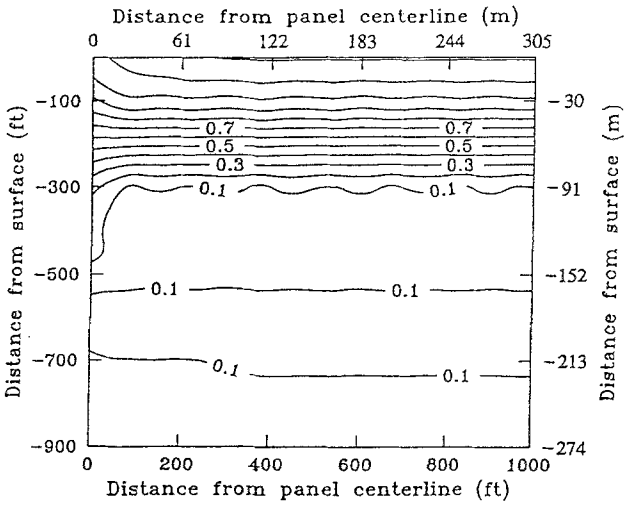

Fig. 7. Normalized pre-mining hydraulic conductivity

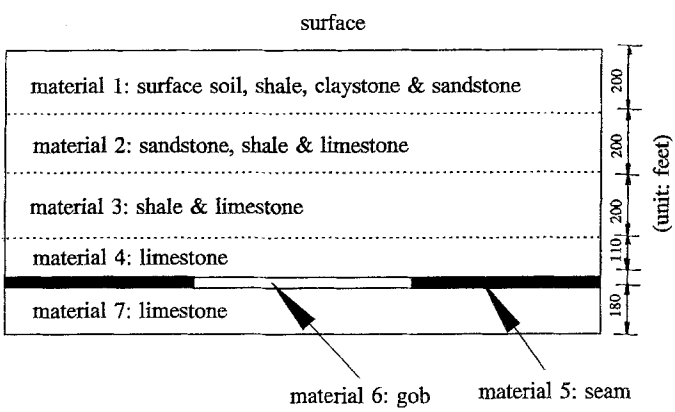

Fig. 8. Strata lithology over a panel

Table 1. Parameters for the finite element model

Material	Conductivity (gpd/ft^2)	Modulus (psf)	Poisson ratio
1	4.20	250000	0.27
2	0.40	850000	0.18
3	0.40	460000	0.22
4	1.10	460000	0.22
5	0.50	200000	0.37
6	0.30	10000	0.40
7	0.80	500000	0.20

Conversion: 1 gpd/ft^2 = 4.72×10^{-7} m/s and 1 psf = 47.88 Pa

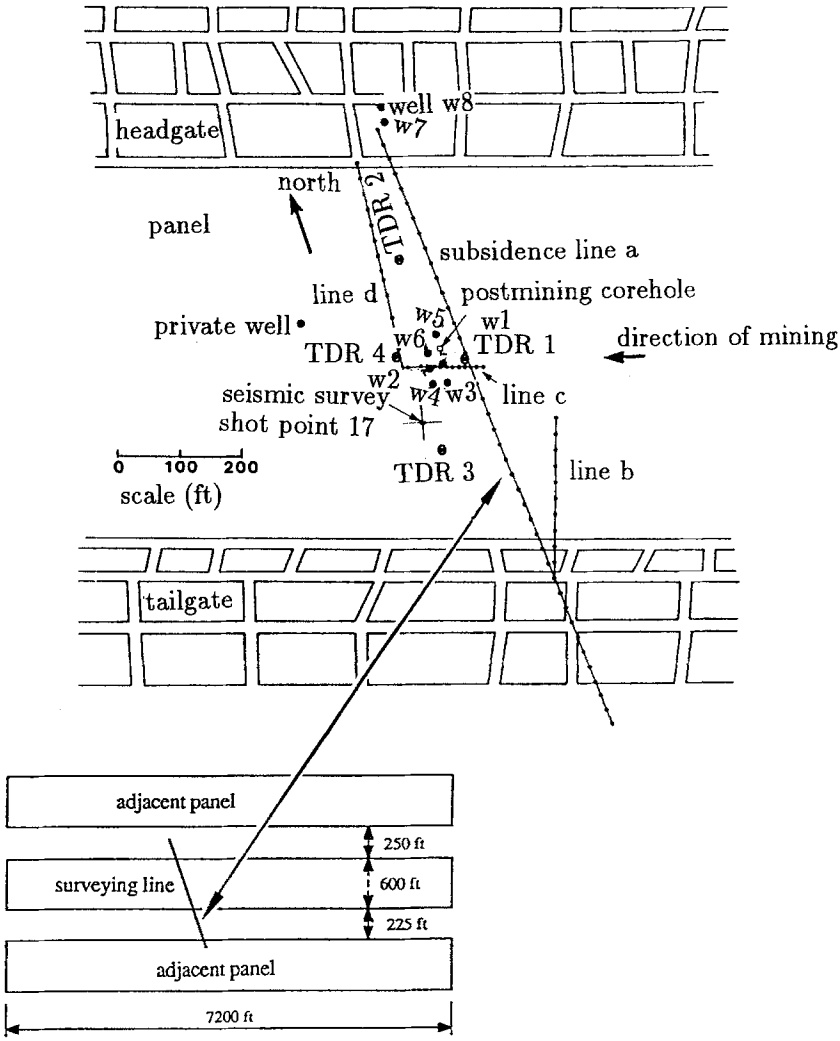

Fig. 9. Layout of mine panels

representing the pre-mining hydraulic regime. A force boundary condition equivalent to overburden load is applied at the mining level. The stress and flow boundary conditions are also illustrated in Fig. 10.

7.1 Analysis of Strata Subsidence

The form and magnitude of surface subsidence may be determined from the measured deformation field. The equilibrium form (long term) of the subsidence profile may be used to confirm the appropriateness of the elastic parameters used in the analysis. These elastic parameters are then used in the numerical model to further aid in determining the subsequent modification in hydraulic conductivities and the resulting change in the fluid flux field.

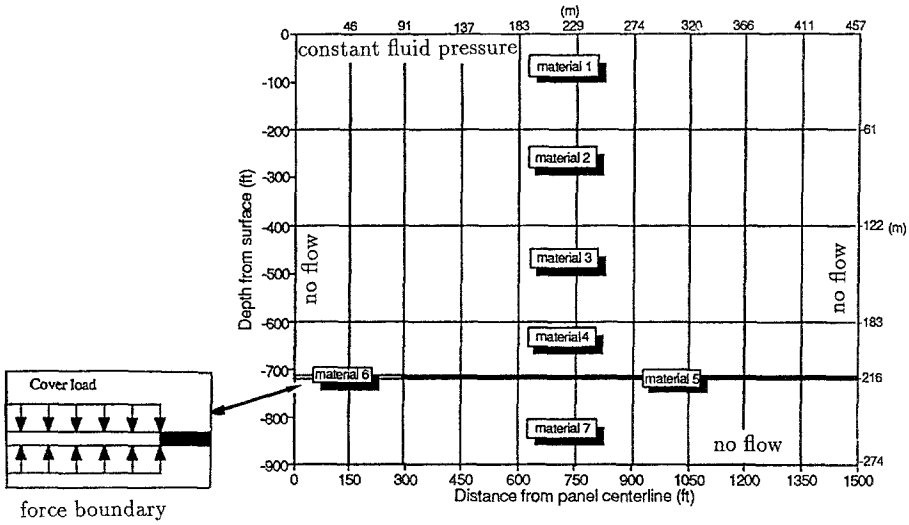

Fig. 10. Finite element layout

The mining-induced subsidence field, determined through use of the model, is illustrated in Figs. 11 and 12 for magnitudes of the pore pressure coefficient α between 0.5 and 1. It is apparent that mining-induced pore pressure magnitudes exercise significant influence over the resulting subsidence field. As α increases towards unity, the subsidence magnitude correspondingly increases. The difference in subsidence for different α is more explicitly expressed by surface subsidence profiles as illustrated in Fig. 13 for α values from 0.1 to 1, where the measured normalized surface subsidence is included for comparison. It is of interest to note that significant variation occurs as α is reduced from 1.0 to 0.1, but that the process appears linear, as would be expected. This is a result of the corresponding increase

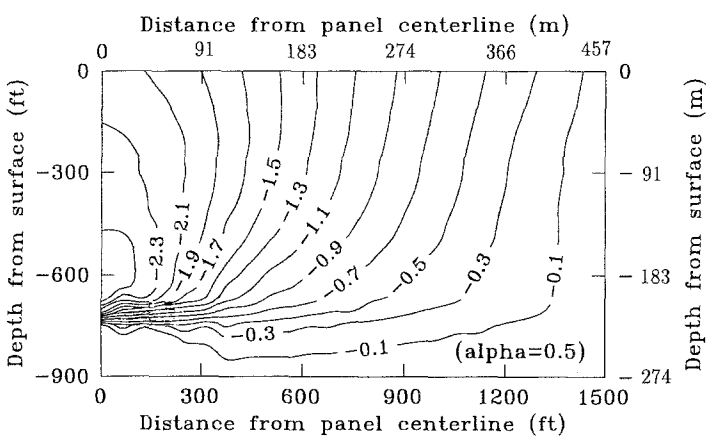

Fig. 11. Subsidence contour ($\alpha = 0.5$)

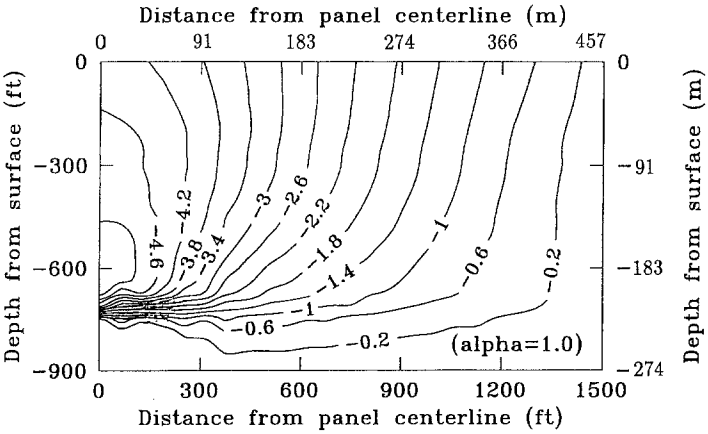

Fig. 12. Subsidence contour ($\alpha = 1.0$)

in seepage force in the porous medium as α increases. It is important to note that the illustrated range of α extends beyond the reasonable limits of 1.0 to 0.7, representative of sedimentary rocks. The second observation is that, in comparison with the influence of the gravity load, the change in pore pressure has a dominant influence on the magnitude of surface subsidence, representing a significant effect of seepage force (or pressure gradient) over the deformation field under given conditions. The third observation is that the measured subsidence profile closely follows the subsidence predicted by $\alpha = 0.1$ over the seam area, while the

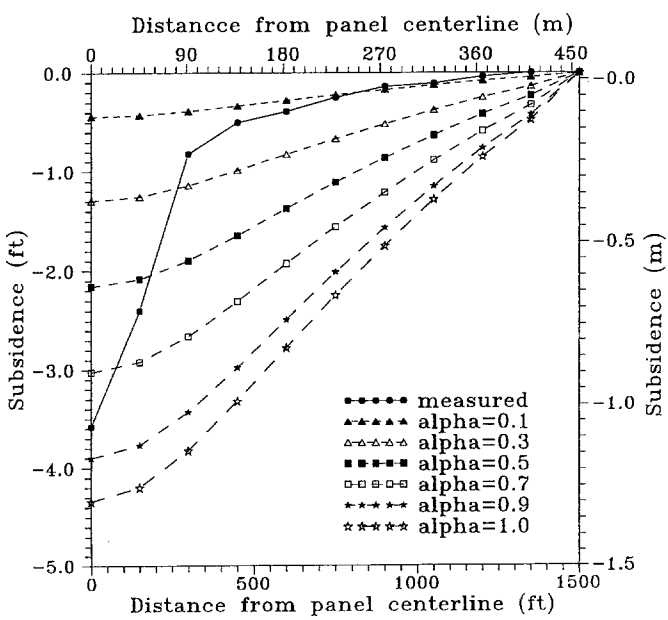

Fig. 13. Measured and calculated subsidence with various α

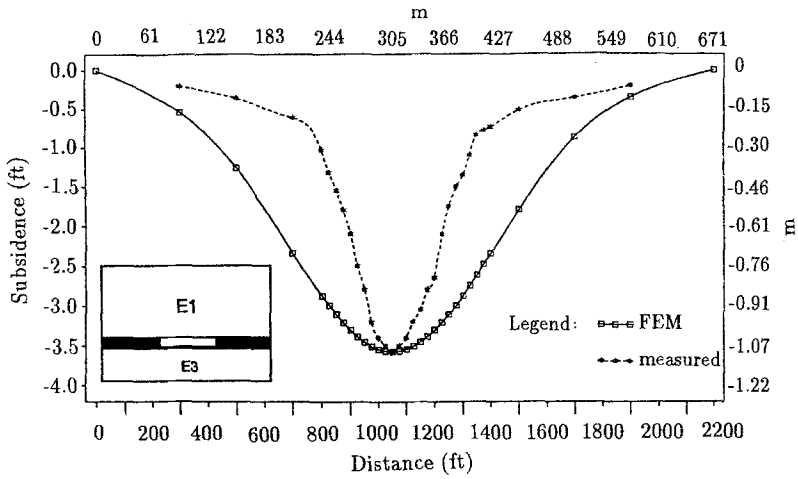

Fig. 14. Comparison of calculated and measured subsidence (a)

maximum subsidence magnitude is comparable to the subsidence with $\alpha = 0.8$. However, the measured surface subsidence shows a steep subsidence profile over the panel, which significantly deviates from the calculated subsidence profiles. This deviation may be attributed to the heterogeneous material properties that develop in the overlying strata, as a result of the nonlinear response to mining induced strains, which are in contrast to the homogeneous and linear finite element modeling. As an example, Fig. 14 depicts the comparison of subsidence between the measured and predicted profiles using a mesh where the elastic modulus does not differentiate between that over the seam and that over the gob. The noticeable discrepancy between the two is apparent. However, if the elastic modulus over the

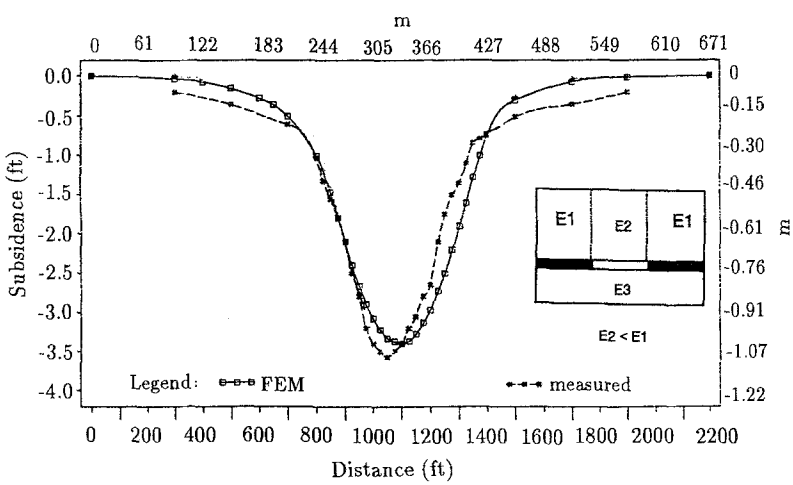

Fig. 15. Comparison of calculated and measured subsidence (b)

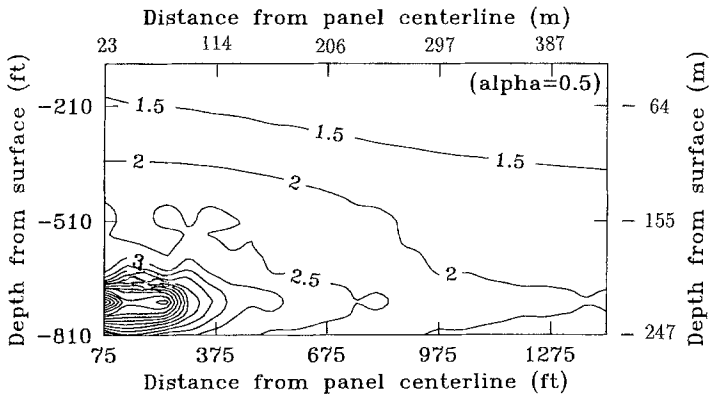

Fig. 16. Ratio of conductivity (K/K_0) in intact rock ($\alpha = 0.5$)

gob is modified to simulate the influence of mining, then a more favorable match is allowed, as shown in Fig. 15.

7.2 Variation of Hydraulic Conductivity

Once the deformation field within the mining region is determined, stress-dependent magnitudes of dimensionless hydraulic conductivity can be evaluated from Eq. (24) for intact rock, or from Eq. (30) for fractured rock.

If Eq. (24) is used for intact rock, effective stresses are calculated from Eq. (13) after stresses and pore pressure distributions are obtained from the finite element analysis. The distribution of dimensionless hydraulic conductivity is illustrated in Figs. 16 and 17, where the pore pressure coefficients, α, are assumed as 0.5 and 1, respectively. These represent extreme bounding magnitudes for sedimentary rocks, where values of the pore pressure parameter are typically in the range 0.7 to 1.0. The immediate observation is that little change in hydraulic conductivity has taken

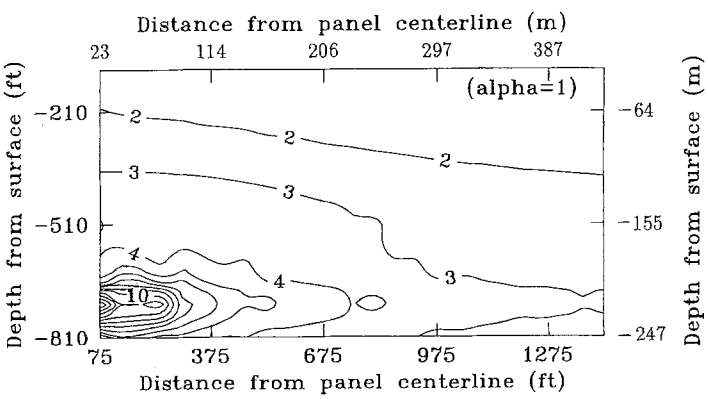

Fig. 17. Ratio of conductivity (K/K_0) in intact rock ($\alpha = 1.0$)

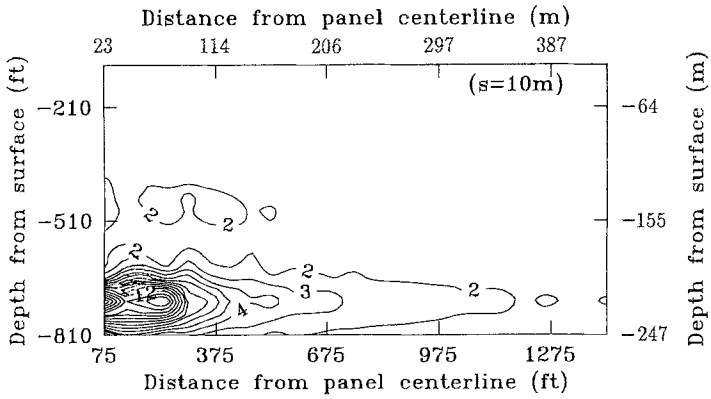

Fig. 18. Ratio of conductivity (K/K_0) in fractured rock ($s = 10$ m)

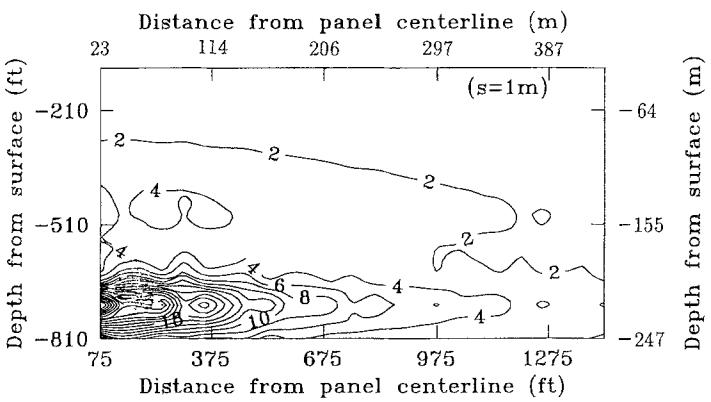

Fig. 19. Ratio of conductivity (K/K_0) in fractured rock ($s = 1$ m)

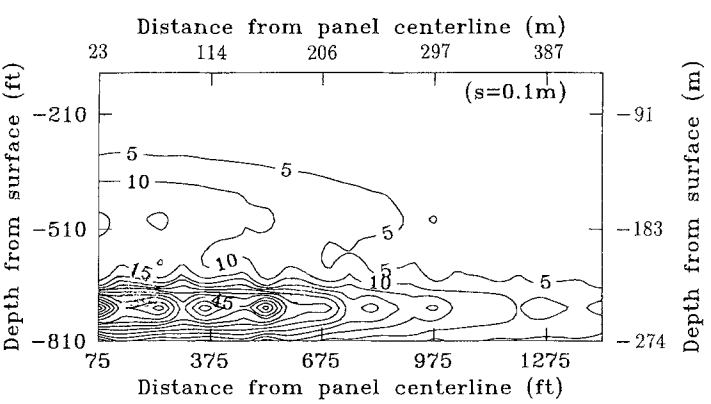

Fig. 20. Ratio of conductivity (K/K_0) in fractured rock ($s = 0.1$ m)

place in the near surface strata, in contrast to the more radical changes that have occurred in close vicinity to the mining panel, especially in the caving or severely fractured zones. In general, a higher pore pressure coefficient results in a greater change in hydraulic conductivity.

For fractured rock, Figs. 18, 19 and 20 depict the profiles of the ratio of post-mining to pre-mining hydraulic conductivities where the pore pressure coefficient, α, is 0.5 and fracture spacings are 10 m (32.8 ft), 1 m (3.28 ft), and 0.1 m (0.33 ft), respectively. The change in hydraulic conductivity is manifest primarily in the vicinity of the mining panel. As apparent in Eq. (30), changes in hydraulic conductivity in fractured rock strongly depend on fracture spacing and strata deformation, in addition to the secondary influence of the mechanical properties of rock and fractures.

The ratios of post-mining to pre-mining hydraulic conductivities close to the centerline of the panel for both the intact rock model and fractured rock models are compared (Fig. 21). In the region immediately above the mining panel, greater changes in hydraulic conductivity occur in the fractured medium than in the intact medium. The difference of the changes in hydraulic conductivity between the fractured medium and the intact medium increases dramatically as the fracture spacing decreases. This results from mining-induced strain being distributed over fewer fractures with a corresponding (relatively) greater change in aperture.

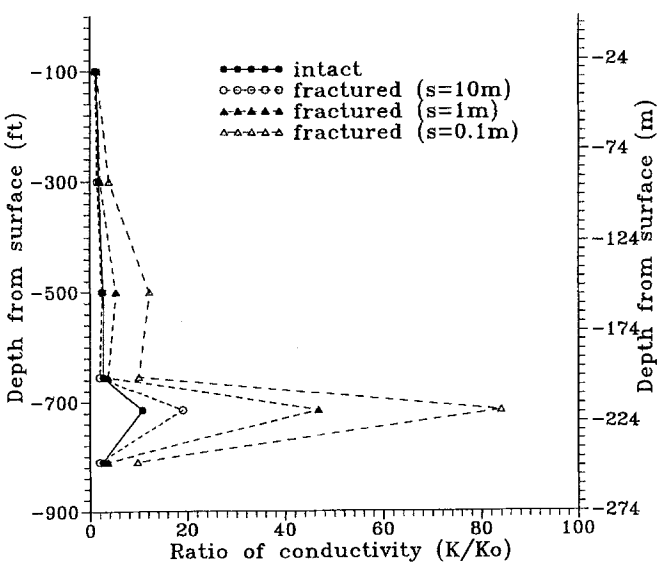

Fig. 21. Ratio of conductivity close to panel centerline

It is of importance to compare the modeling results with field measurements. In the case study examined here, the pre-mining and post-mining hydraulic conductivities were determined by falling head permeability, slug, pumping test and

borehole packer tests (Hasenfus et al., 1988). The packer tests conducted in the post-mining borehole indicated both increasing and decreasing conductivities relative to pre-mining values. Unfortunately, due to severe rock failure over the mined panel area, no observation was available within 130 feet (40 m) above the panel. Comparisons of the ratio of post-mining to pre-mining hydraulic conductivity above the panel centerline among the models of fractured rock and intact rock and the measurement, as available, are shown in Fig. 22. The measured results indicate the oscillatory variation of the conductivity as depth increases, which may be due to the effect of shear slippage between strata layers under mining influence, and localized heterogeneities of deformation. As apparent in Eq. 33, additional changes in hydraulic conductivity may occur as a result of the shearing between layers. The slightly larger change in the ratio of hydraulic conductivity for the intact rock model, over that of the model representing fractured rock, is limited to shallow depths and where the fracture spacing is 10 m.

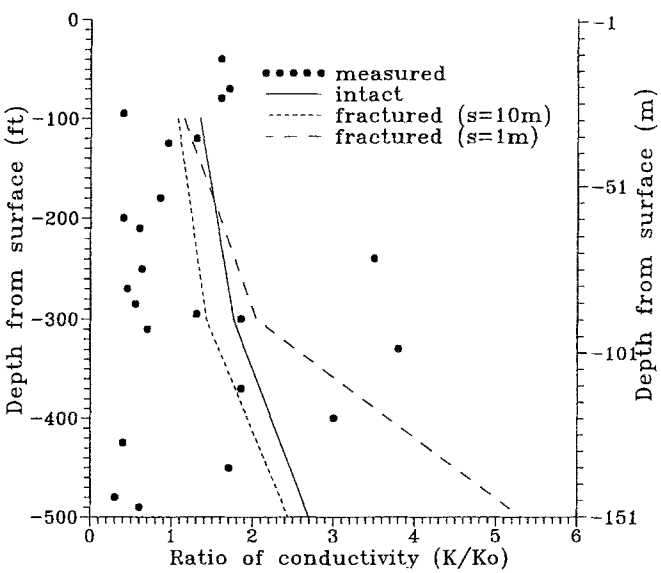

Fig. 22. Ratio of conductivity between models and measurement.

Since fracture apertures are evaluated from the defined spacing and measured initial conductivity, it is observed that, at greater depth, the predicted change of hydraulic conductivity by the fractured rock model tends to be greater than the measured magnitude. This mismatch is conditioned by the choice of fracture spacing, consequently, a smaller spacing would result in a closer match. This adjustment is not contemplated, rather the natural uncertainty of parameters is retained in the model. The better correspondence between the measured data and the prediction by the intact rock model, and the fractured rock model with large fracture spacing, than with the model using small fracture spacing reflects the domination of the original permeability distribution, i.e. the permeability decreases with depth.

8. Conclusions

This paper provides a variety of models for evaluating deformation and enhancement of hydraulic conductivity in both intact and in fractured strata. Although not limited to this, the models are applied to describe the change in hydraulic behavior that accompanies longwall mining. The models are based on the theory of coupled steady-state poroelasticity where the displacement and fluid pressure fields are obtained through finite element analysis. For intact rock, changes in hydraulic conductivity are determined using the concept of grain size analysis, via a theory of elastic contact. For fractured rock, changes in hydraulic conductivity are evaluated through the parallel plate description in an equivalent porous medium. In both cases, the stress state of the porous medium exercises critical influence on the variation of hydraulic conductivity.

In applying the model, it is observed that the magnitude of the subsidence field over the mining panel is strongly controlled by the induced pore pressures. This results from the choice of force boundary conditions at the panel, rather than the prescribed displacement conditions, that would yield a more uniform subsidence profile with changing pore pressure coefficient α. Representative magnitudes the pore pressure parameter, α, are in the range 0.7 to 1.0 for sedimentary rocks, effectively limiting the range of attainable subsidence profiles.

Changes in hydraulic conductivity are directly associated with the changes in stresses and pore pressure magnitudes from the initial pre-mining status. The greatest changes in hydraulic conductivity tend to occur in the vicinity of the mining panel where the surrounding rock is subjected to severe caving or fracturing as a result of stress or deformation variation of the strata. The comparison of changes in hydraulic conductivity, a major concern when mining under aquifers, shows compatible patterns (but different magnitudes) between the fractured rock model and the intact rock model immediately above the mining panel. A consistent trend is evident, to a certain extent, between the results from the models and those from the measurements. Fracture spacing is one of the key factors that controls the intensity of the changes in hydraulic conductivity.

Nomenclature

$\mathbf{A}$	derivatives of shape functions
b_0	initial fracture aperture
b	width of fracture opening
$\mathbf{B}$	strain-displacement matrix
c	constant
d	mean grain size or hydraulic radius
$\mathbf{D}$	elasticity matrix
E	elastic modulus
E_0	effective grain modulus
f	boundary tractions
$F(n)$	porosity factor
$\mathbf{F}$	vector of applied boundary tractions
g	gravitational acceleration
n	porosity
$\mathbf{N}$	vector of element shape functions
p	pore pressure
$\mathbf{Q}$	vector of prescribed nodal fluxes
$\mathbf{R_c}$	coupling matrix
R	grain radius
s	fracture spacing
u	displacement
u_f	fracture displacement
u_s	solid displacement
u_t	total displacement
v_i	Darcy's velocity
V	volume of the integral domain

G	shear modulus	α	pore pressure coefficient
$\mathbf{G_s}$	stiffness matrix	δ_{ij}	Kronecker's delta
$\mathbf{G_f}$	conductance matrix	∇	del operator
H	Biot constant	ϕ_d	dilatation angle
k	permeability	μ	fluid dynamic viscosity
K	hydraulic conductivity	ν	Poisson ratios
$\mathbf{K}$	hydraulic conductivity matrix	γ	shear strain
K_0	initial hydraulic conductivity	ϵ_{ij}	strain tensor
K_g	bulk modulus of solid grains	ϵ_{kk}	volumetric strain
K_s	bulk modulus of porous media	σ_{ij}^e	effective stress tensor
K_n	stiffness of fracture	σ_{ij}	stress tensor
K_{sh}	shear stiffness	$\sigma_{kk}/3$	$trace(\sigma_{ij})/3$ = mean stress σ_c
$\mathbf{m}$	one dimensional vector, $= \{1\ \ 1\ \ 0\}^T$		

Appendix

Hydraulic conductivity may be directly related to pore dimension, frequently defined in terms of the hydraulic radius (Scheidegger, 1957). In the well-known theory of Kozeny (Kozeny, 1927), the porous medium is represented by an assemblage of capillaries, of various cross-sections, where the Navier-Stokes equations are solved individually, for each of the parallel arrangement. The hydraulic conductivity is given as

$$K = cn^3 d^2 \left(\frac{\rho g}{\mu}\right), \tag{40}$$

where c is a constant representing the mean size and shape of the grains, and n is porosity.

Comparing Eq. (14) with Eq. (40), it is apparent that porosity is an important factor. Real porous media are comprised of a mixture of large and small particles that may be uncemented or cemented. The porosity of consolidated materials depends mainly on the degree of cementation, while the porosity of unconsolidated materials depends on the packing of the grains, their shape, arrangement and size distribution.

Porosity may have an important control over hydraulic conductivity with hydraulic conductivity increasing with increased porosity. Kozeny-Karman (Bear, 1972) proposed an equation similar to Eq. (40) which includes a factor representing porosity as

$$K = \frac{n^3}{(1-n)^2} \frac{d^2}{180} \left(\frac{\rho g}{\mu}\right), \tag{41}$$

where n is porosity. This equation attempts to incorporate the influence of grain packing on hydraulic conductivity. Alternatively, packing may be incorporated directly for Hubbert's equation as shown in Eq. (14), enabling direct relationships to be established for permeability changes.

The influence of pore pressures on effective stresses is controlled through the pore pressure coefficient α of Eq. (7), which has been experimentally defined by Geertsma (1957) and Skempton (1960) and confirmed from theory by Nur and Byerlee (1971).

Scheidegger (1957) claimed that the hydraulic conductivity of a medium was solely a function of the total external stresses, expressed as a change of pore space under external loading. By carrying out laboratory tests on intact and jointed Barre granite, Kranz et al. (1979) proposed the following equation to predict the change of permeability, k, as a function of difference between confining stress σ_c and pore pressure p as

$$k \propto -\left(\sigma_c - \frac{b}{a} p\right), \tag{42}$$

where b and a are constants representing the effective proportionality of the fluid pressure. Based on the experimental results, Kranz et al. suggested that $b/a < 1$ for jointed rock and $b/a \approx 1$ for intact rock. They also reported a one to two order of magnitude difference between the permeability of jointed rock and that of intact rock at low effective stresses, and almost no difference at high effective stresses.

An empirical formula relating hydraulic conductivity to effective stress is given by Walsh (1981) as

$$K = K_0 \left\{ 1 - (\sqrt{2}\xi) \ln\left(\frac{\sigma_e}{\sigma_e^0}\right) \right\}^3, \tag{43}$$

where K_0 is the initial hydraulic conductivity, σ_e^0 is the initial effective stress, ξ is a factor related to the fracture geometry, and acting effective stress, σ_e, may be estimated from Eq. (13).

Acknowledgements

This work is supported, in part, by the Pennsylvania Energy Development Authority, the Consolidation Coal Company (Consol) and the Nation Science Foundation under grant number MSS-9209059. This support is gratefully acknowledged. This work could not have been completed without the cooperation of the R & D office of Consol, and the willingness of the staff to share data. This opportunity is gratefully acknowledged. The authors also thank two anonymous reviewers and the Editor for providing critical comments and constructive suggestions in revising the manuscript.

References

Barton, N., Bandis, S., Bakhtar, K. (1985): Strength, deformation and conductivity coupling of rock joints. Int. J. Rock Mech. Min. Sci. Geomech. Abstr. 22(3), 121–140.

Bear, J. (1972): Dynamics of fluids in porous media. American Elsevier Pub., Boulder, 764 pp.

Biot, M. A. (1941): General theory of three dimensional consolidation. J. Appl. Phys. 12, 155–164.

Brandt, H. (1955): A study of the speed of sound in porous granular media. J. Appl. Mech. 22, 479–486.

De Wiest (ed.) (1969): Flow through porous media, Academic Press, London, 530 pp.

Einstein, H. H., Dowding, C. H. (1981): Shearing resistance and deformability of rock joints. In: Touloukian, Y. S., Judd, W. R., Roy, R. F. (eds.), Physical properties of rocks and minerals, McGraw-Hill, New York, 177–220.

Elsworth, D. (1989): Thermal permeability enhancement of blocky rocks: one dimensional flows. Int. J. Rock Mech., Min. Sci. Geomech. Abstr. 26(3/4), 329–339.

Elsworth, D., Xiang, J. (1989): A reduced degree of freedom model for thermal permeability enhancement in blocky rock. Geothermics 18, 691–709.

Freeze, R. A., Cherry, J. A. (1979): Groundwater. Prentice-Hall, Englewood Cliffs, 604 pp.

Gale, J. E. (1982): The effects of fracture type (induced versus natural) on the stress-fracture closure-fracture permeability relationship. 23rd U.S. Rock Mech. Symp., Univ. of California, Berkeley, 290–298.

Gangi, A. F. (1978): Variation of whole and fractured porous rock permeability with confining pressure. Int. J. Rock Mech. Min. Sci. Geomech. Abstr. 15(3), 249–257.

Geertsma, J. (1957): The effect of fluid pressure decline on volumetric changes of porous rocks. Trans. AIME, 331.

Hasenfus, G. J., Johnson, K. L., Su, D. W. H. (1988): A hydrogeomechanical study of overburden aquifer response to longwall mining. In: Proc., 7th Int. Conf. Ground Control in Mining, Morgantown, WV, 149–162.

Hoek, E., Bray, J. W. (1977): Rock slope engineering, 2nd edn., Inst. Min. and Metall., London, 402 pp.

Hubbert, M. K. (1940): The theory of ground water motion. J. Geol. 48, 785–944.

Iwai, K. (1976): Fundamental studies of fluid flow through a single fracture. Ph.D. Dissertation, University of California, Berkeley, 268 pp.

Jones, F. O. (1975): A laboratory study of the effects of confining pressure on fracture flow and storage capacity in carbonate rocks. J. Petrol. Technol. 21–27.

Kozeny, J., Ber, S. (1927): Wiener Akad, Abt. 2a, 136, 271.

Kranz, R. L., Frankel, A. D., Engelder, T., Scholz, C. H. (1979): The permeability of whole and jointed Barre granite. Int. J. Rock Mech. Min. Sci. Geomech. Abstr. 16(3), 225–234.

Krumbein, W. C., Monk, G. D. (1943): Permeability as a function of the size parameters of unconsolidated sand. Trans. Am. Inst. Min. Metall. Petrol. Engng. 151, 153–163.

Louis, C. (1969): Groundwater flow in rock masses and its influence on stability. Rock Mech. Res. Report 10, Imperial College, UK.

Nur, A., Byerlee, J. D. (1971): An exact effective stress law for elastic deformation of rock with fluids. J. Geophys. Res. 76(26), 6414–6419.

Robin, P. Y. F. (1973): Note on effective pressure. J. Geophys. Res. 78(14), 2434–2437.

Rosso, R. S. (1976): A comparison of joint stiffness measurements in direct shear, triaxial compression, and in situ. Int. Rock Mech. Min. Sci. Geomech. Abstr. 13, 167–172.

Scheidegger, A. E. (1957): The physics of flow through porous media. Macmillan, New York, 236 pp.

Skempton, A. W. (1960): Effective stress in soils, concrete and rock. Pore pressure and suction in soils, Butterworths, London.

Snow, D. T. (1968): Rock fracture spacings, openings, and porosities. J. Soil Mech. Found Div., Proc. ASCE 94, 73–91.

Terzaghi, K. V. (1923): Die Berechung der Durchlässigkeitsziffer des Tones aus dem Verlauf der hydrodynamischen Spannungserscheinungen. Sitzungsber. Akad. Wiss. Wien Math Naturwiss. Kl. Abt. 2A, 132, 105.

Timoshenko, S. (1934): Theory of elasticity, 1st edn., McGraw-Hill, New York 416 pp.

Walsh, J. B. (1981): Effect of pore pressure and confining pressure on fracture permeability. Int. Rock Mech. Min. Sci. Geomech. Abstr. 18(3), 429–435.

Warren, J. E., Root, P. J. (1963): The behavior of naturally fractured reservoirs. J. Soc. Pet. Eng. 3, 245–255.

Witherspoon, P. A., Wang, J. S. Y., Iwai, K., Gale, J. E. (1980): Validity of Cubic law for fluid flow in a deformable rock fracture. Water Resour. Res. 16(6), 1016–1024.

Young, A., Low, P. F., Mclatchie, A. S. (1964): Permeability studies of argillaceous rocks. J. Geophys. Res. 69, 4237–4245.

Authors' address: Dr. Mao Bai, The University of Oklahoma, Energy Center T301, 100 East Boyd, Norman, OK 73019-0628, U.S.A.